

MODELING THE FIELD OF A PASSIVE SCALAR IN A NONISOTHERMAL TURBULENT
PLANE GAS JET

V. N. Abrashin, V. N. Barykin,
O. G. Martynenko, and E. V. Radkevich

UDC 532.517.4

On the basis of a second-order correlational model of turbulence and an effective numerical algorithm, the problem of the distribution of thermal characteristics in a planenonisotheermal turbulent gas jet is solved.

Free turbulent shear flows, such as turbulent jets, represent a sufficiently general form of flow with a widerange of applications. The system of accurate equations describing all the details of the evolution of the velocity field and the scalar fields cannot be solved using current computational means. Therefore, special interest attaches to models that are suitable for practical calculations. Sufficient accuracy usually depends on the conditions of the specific problem.

Formulation of the Problem

A gas jet of velocity u_0 and temperature T_0 at the nozzle outlet leaves a nozzle of transverse dimension d considerably smaller than the longitudinal dimension α into the atmosphere, or in the more general case into a cotraveling flow of velocity u_c . It is required to calculate the dynamic and thermal characteristics of the jet in the case of large Reynolds numbers and a small temperature difference, allowing heat to be regarded as a passive impurity, in the range of jet cross sections 20-100 caliber, and to compare the results with experiment.

For a plane jet in the boundary-layer approximation, the mean velocity is described by the continuity equation and an equation following from the law of momentum conservation

$$(\alpha + u) \frac{\partial u}{\partial x} + w \frac{\partial u}{\partial z} = \frac{\partial}{\partial z} \left(\beta \frac{\partial u}{\partial z} - R_{12} \right).$$

The velocity distribution depends significantly on the law of variation in Reynolds stress $u_i u_j$, since the low pressure gradient means that it is equilibrium only with inertial forces. It has been shown in numerous works that the predominant Reynolds-stress term is $u_1 u_2 = R_{12}$. Correspondingly, only one equation is used for the Reynolds stress

$$(\alpha + u) \frac{\partial R_{12}}{\partial x} + w \frac{\partial R_{12}}{\partial z} = \frac{\partial}{\partial z} \left[\left(\beta + a_1 \frac{E^2}{D_u} \right) \frac{\partial R_{12}}{\partial z} \right] + a_2 E \frac{\partial u}{\partial z} + a_3 \frac{D_u}{E} R_{12}.$$

Twice the kinetic energy of turbulence E and its rate of dissipation D_u appear in the equation as unknowns. The equation for E in the present case is written in the form

$$(\alpha + u) \frac{\partial E}{\partial x} + w \frac{\partial E}{\partial z} = \frac{\partial}{\partial z} \left[\left(\beta + b_1 \frac{E^2}{D_u} \right) \frac{\partial E}{\partial z} \right] + b_2 R_{12} \frac{\partial u}{\partial z} + b_3 D_u.$$

The following differential equation is used for the dissipation rate of the kinetic energy of turbulence

$$(\alpha + u) \frac{\partial D_u}{\partial x} + w \frac{\partial D_u}{\partial z} = \frac{\partial}{\partial z} \left[\left(\beta + c_1 \frac{E^2}{D_u} \right) \frac{\partial D_u}{\partial z} \right] + c_2 R_{12} \frac{D_u}{E} \frac{\partial u}{\partial z} + c_3 \frac{D_u^2}{E},$$

where α_i, b_i, c_i are phenomenological constants.

A. V. Lykov Institute of Heat and Mass Transfer, Academy of Sciences of the Belorussian SSR. Institute of Mathematics, Academy of Sciences of the Belorussian SSR, Minsk. Translated from *Inzhenerno-Fizicheskii Zhurnal*, Vol. 54, No. 3, pp. 387-393, March, 1988. Original article submitted January 27, 1987.

This system of equations is conventional; it has been tested for many problems and gives results in agreement with experiment (relative error of the order of 5-15%).

The mean temperature T is determined by the equation

$$(\alpha + u) \frac{\partial T}{\partial x} + w \frac{\partial T}{\partial z} = \frac{\partial}{\partial z} \left(\gamma \frac{\partial T}{\partial z} - R_{2T} \right) - \frac{\partial R_{1T}}{\partial x}.$$

In the general case, its distribution depends significantly on the components of the heat flux $u_i t$, since it is in equilibrium with the inertial terms of the equation. In the case considered here, the terms $u_1 t = R_{1T}$ and $u_2 t = R_{2T}$ play an important role. The corresponding equations are sufficiently complex, but it is known from experiments [1] that the behavior of R_{1T} is largely analogous to that of R_{2T} . Therefore, the heat flux is calculated from the equation for R_{2T} , since the components appearing there have been more completely tested experimentally

$$(\alpha + u) \frac{\partial R_{2T}}{\partial x} + w \frac{\partial R_{2T}}{\partial z} = \frac{\partial}{\partial z} \left[\left(\gamma + l_1 \frac{E^2}{D_u} \right) \frac{\partial R_{2T}}{\partial z} \right] + l_2 E \frac{\partial T}{\partial z} + l_3 \frac{D_u}{E} R_{2T}.$$

The relation between R_{1T} and R_{2T} is determined by an analytical expression. For the mean square temperature pulsations $t^2 = \theta$, an equation obtained from the accurate equation in the three-moment approximation according to [2] is employed

$$(\alpha + u) \frac{\partial \theta}{\partial x} + w \frac{\partial \theta}{\partial z} = \frac{\partial}{\partial z} \left[\left(\gamma + m_1 \frac{E^2}{D_u} \right) \frac{\partial \theta}{\partial z} \right] + m_2 R_{2T} \frac{\partial T}{\partial z} - 2R_{1T} \frac{\partial T}{\partial x} + m_3 D_T.$$

The dissipation rate of the temperature pulsations D_T is specified on the basis of the following relation, which agrees with experiment

$$D_T = R \frac{\theta}{E} D_u.$$

In the given equations, l_i , m_i , and R are phenomenological constants.

The initial conditions for ΔT and u are approximated by the experimental dependences

$$\Delta T = \Delta T_m \operatorname{sech}^2(0,881 \xi_t), \quad \Delta T_m = \Delta T_0 [0,267(x/h - 1)]^{-1/2}, \\ u = u_m \operatorname{sech}^2(0,881 \xi_u), \quad u_m = u_0 [0,174(x/h - 1)]^{-1/2},$$

where $\xi_u = z/0,109(x/h + 1,17)$, $\xi_t = z/0,141(x/h + 3,5)$. For R_{12} , E , R_{2T} , and θ , expressions obtained from the approximation of the experimental data for $x/h = 40$ are used

$$\theta = \Delta T_m^2 \cdot 10^{-2} [27,29 \exp(-0,853 \xi_t^2) - 24,44 \exp(-1,186 \xi_t^2)], \\ R_{2T} = u_m \Delta T_m \cdot 10^{-2} [3,896 \exp(-0,326 \xi_t^2) - 3,691 \exp(-7,136 \xi_t^2)], \\ R_{12} = u_m^2 \cdot 10^{-2} [4,629 \exp(-0,804 \xi_u^2) - 3,978 \exp(-2,626 \xi_u^2)], \\ E = 2,7 u_m^2 \cdot 10^{-2} [9,797 \exp(-0,568 \xi_u^2) - 5,923 \exp(-1,831 \xi_u^2)].$$

The boundary conditions are specified in the form

$$z = 0: \frac{\partial u}{\partial z} = 0, \quad R_{12} = 0, \quad \frac{\partial E}{\partial z} = 0, \quad \frac{\partial D_u}{\partial z} = 0; \\ z = z_m: u = u_{bo}, \quad R_{12} = R_{12bo}, \quad E = E_{bo}, \quad D_u = D_{uboi}; \\ z = 0: \frac{\partial T}{\partial z} = 0, \quad R_{2T} = 0, \quad \frac{\partial \theta}{\partial z} = 0, \quad \frac{\partial D_T}{\partial z} = 0; \\ z = z_m: T = T_{in}, \quad R_{2T} = R_{2Tbo}, \quad \theta = \theta_{bo}, \quad D_T = D_{Tbo}.$$

The expansion of the jet is determined by the condition

$$|\partial u / \partial z| z_m \leq 10^{-2} u_m / z_m.$$

Analogously, the expansion of the thermal boundary is determined in terms of T_m .

Numerical Algorithm

On account of the nonlinearity of the system of equations and the presence of small parameters, the accuracy of the calculation depends largely on the numerical algorithm. Its basic features are illustrated in the model equation

$$\frac{\partial \varphi}{\partial x} + k(\varphi) \frac{\partial \varphi}{\partial z} = \mu \frac{\partial^2 \varphi}{\partial z^2}. \quad (1)$$

A uniform rectangular grid is used

$$\begin{aligned} \omega_{h_x h_z}^{\alpha_0} &= \{x_j = x_0 + j h_x, j = 0, 1, \dots, N_x; \\ z_i &= i h_z, i = 0, 1, \dots, N_z; h_x = h_z / \alpha_0\} \end{aligned}$$

as well as a difference scheme of the form [3]

$$\frac{\hat{\varphi}_i - \varphi_{i-s}}{h_x} + \sigma_1 (\hat{k}_i^+ \hat{\varphi}_{z,i}^- + \hat{k}_i^- \hat{\varphi}_{z,i}) + (1 - \sigma_1) (k_{i-s}^+ \varphi_{z,i-s}^- + k_{i-s}^- \varphi_{z,i-s}) = \mu (\sigma_2 \hat{\varphi}_{zz,i} + (1 - \sigma_2) \varphi_{zz,i-s}), \quad (2)$$

$$\varphi_i = \varphi(x_j, z_i), \quad \hat{\varphi}_i = \varphi(x_{j+1}, z_i), \quad k_i = k(\varphi_i), \quad s = \text{sign } k_i,$$

$$k_i^+ = (k_i - s\alpha_0 + |k_i - s\alpha_0|)/2 \geq 0, \quad k_i^- = (k_i - s\alpha_0 - |k_i - s\alpha_0|)/2 \leq 0.$$

Here $0 \leq \sigma_1, \sigma_2 \leq 1$ are weighting functions.

The first differential approximation of the first-order difference scheme takes the form

$$\frac{\partial \varphi}{\partial x} + k \frac{\partial \varphi}{\partial z} = (\mu + \tilde{\mu}) \frac{\partial^2 \varphi}{\partial z^2}, \quad (3)$$

where $\sigma_1 = 0$, $\tilde{\mu} = 0,5 h_x (k - s\alpha_0) ((s_1 + s)\alpha_0 - k)$; $\sigma_1 = 1$, $\tilde{\mu} = 0,5 h_x (\hat{k} - s\alpha_0) ((s_1 - s)\alpha_0 + \hat{k})$, $s_1 = \text{sign}(k - s\alpha_0)$. Since $\tilde{\mu} > 0$, the solution has a monotonic structure for stable difference schemes [4]. The quality of the method is best when the schematic viscosity μ is a minimum. In practice, μ is minimized by the choice of the parameter α_0 .

When $\sigma_1 = 1$, the difference scheme in Eq. (2) is nonlinear, and thus an iteration process of the following form is necessary

$$\frac{\varphi_i^{l+1} - \varphi_{i-s}^l}{h_x} + k_i^{l+1} \varphi_{z,i}^{l+1} + \hat{k}_i^{l+1} \varphi_{z,i}^{l+1} = \mu \varphi_{zz,i}^{l+1}, \quad (4)$$

where $k_i^l = k(\varphi^l)$. For the error $\rho = \varphi^{l+1} - \hat{\varphi}$, where $\hat{\varphi}$ is the accurate solution of Eq. (2), it is found that $\|\rho\| \leq c h_x \|\rho\|^l$. Convergence occurs if $c h_x < 1$, where $c = \max |-\partial k(\tilde{\varphi}^l) / \partial \varphi \hat{\varphi}_z|$ when $s_1 = 1$; $c = \max |-\partial k(\tilde{\varphi}^l) / \partial \varphi \hat{\varphi}_z|$, $s_1 = -1$; $\tilde{\varphi}^l = \varphi + \theta(\varphi - \hat{\varphi})$, $0 \leq \theta \leq 1$, $\tilde{\varphi}$ is the mean value.

In contrast to model Eq. (1), the initial physical problem includes a term of the form

$$\frac{\partial}{\partial z} \left(\frac{E^2}{D_u} \frac{\partial \varphi}{\partial z} \right)$$

which is approximated as follows

$$1/h_y^2 (\hat{a}_{i+1} (\hat{\varphi}_{i+1} - \hat{\varphi}_i) - \hat{a}_i (\hat{\varphi}_i - \hat{\varphi}_{i-1})).$$

Consider the model functionals

$$\begin{aligned} \text{a) } a_i &= E_i^2 / D_{u,i}; & \text{b) } a_i &= 0,5 (E_i^2 / D_{u,i} + E_{i-1}^2 / D_{u,i}); \\ \text{c) } a_i &= \frac{1}{6} \left(\frac{E_i^2}{D_{u,i}} + \frac{E_{i-1}^2}{D_{u,i-1}} + 2 \frac{(E_i + E_{i-1})^2}{(D_{u,i} + D_{u,i-1})} \right). \end{aligned}$$

Numerical experiment shows that, with sufficiently large grid steps, the use of functionals of the form in (c) allows a more accurate solution to be obtained, and requires less machine time, than the use of the expressions in (a) or (b). The model functionals a_i are nonlinear functions of E, D_u . Therefore, an iterative process based on the following expression is used

$$\begin{aligned} & (u + \alpha_0) \left((\varphi_i - \varphi_{i-s})/h_x + \sigma (k_i^+ \varphi_{z,i}^{i+1} + k_i^- \varphi_{z,i}^{i+1}) + (1 - \sigma) (k_{i-s}^+ \varphi_{z,i-s} + k_{i-s}^- \varphi_{z,i-s}) \right) \\ & = \mu \varphi_{z,i}^{i+1} + (a_{i+1} \varphi_i^{i+1} - a_i (\varphi_{i+1} - \varphi_i) - a_i (\varphi_i - \varphi_{i-1}))/h_z^2. \end{aligned}$$

The difference scheme is linear relative to $\frac{\varphi^{i+1}}{\varphi}$. To solve the system of difference equations in Eq. (3), they are reduced to the form

$$A_i \varphi_{i-1}^{i+1} - C_i \varphi_i^{i+1} + B_i \varphi_{i+1}^{i+1} = -F_i, \quad i = 1, 2, \dots, M-1. \quad (5)$$

The system of algebraic equations in Eq. (5) is solved by the method of difference fitting. In the present case, it is stable, since

$$|C_i| \geq |A_i| + |B_i|.$$

The fitting factors for the functions in Eq. (5) are

$$\begin{aligned} A_i &= \frac{h_x}{h_z^2} (\beta + r_1 a_i) + \sigma h_x (u + \alpha_0) k_i^+, \\ B_i &= \frac{h_x}{h_z^2} (\beta + r_1 a_{i+1}) + \sigma h_x (u + \alpha_0) k_i^-, \\ C_i &= A_i + B_i + (u + \alpha_0) + R_c, \quad F_i = R_\varphi + R_f, \\ R_\varphi &= (\varphi_{i-s} - (1 - \sigma_1) h_x (k_{i-s}^+ \varphi_{z,i-s} + k_{i-s}^- \varphi_{z,i-s})). \end{aligned}$$

The values of R_c and R_f are as follows

$$\begin{aligned} u: R_c &= 0, \quad R_f = 0,5 h_x / h_z (R_{12,i-1} - R_{12,i+1}), \\ R_{12}: R_c &= -h_x a_3 (D_{u,i} / E_i), \quad R_f = 0,5 h_x / h_z a_2 E_i (u_{i+1}^{i+1} - u_{i-1}^{i+1}), \\ E: R_c &= 0, \quad R_f = 0,5 h_x / h_z b_2 R_{12,i} (u_{i+1}^{i+1} - u_{i-1}^{i+1}) + h_x b_3 D_u, \\ D_u: R_c &= -h_x c_3 (D_{u,i} / E_i), \quad R_f = 0,5 h_x / h_z c_2 R_{12,i} (u_{i+1}^{i+1} - u_{i-1}^{i+1}) (D_{u,i} / E_i). \end{aligned}$$

The continuity equation is approximated by a difference equation

$$\frac{\hat{w}_{i+1} - \hat{w}_i}{h_z} = -0,5 \left((u_i - u_i)/h_x + (u_{i+1} - u_{i+1})/h_x \right).$$

The initial conditions are specified by analytical expressions. The boundary conditions when $z = z_0$ are specified from physical considerations. The condition of the first kind at the jet axis is specified accurately, and the derivatives of the form $\partial \varphi / \partial z$ are specified in difference form.

The features of the calculation scheme are as follows. 1. The initial values for calculating the dynamic and thermal characteristics are corrected by additional factors which are different for different cross sections of the jet. 2. The mean square temperature pulsations and kinetic energy close to the axis are determined by expressions of the form

$$E = \begin{cases} E_1, & \xi \leq 0,1, \\ E_2, & \xi \geq 0,1, \end{cases}$$

where

$$E_1 = 2,7 u_m^2 \cdot 10^{-2} [A + 10^2 (\Phi - A) \xi_u^2], \quad E_2 = E_2 \text{ini}.$$

$$\Phi = \frac{1}{2,7} 10^2 u_m^{-2} E_2 |_{\xi_u=0,1}.$$



Fig. 1. Mean temperature: 1) $x/d = 40$; 2) 60; 3) 80.

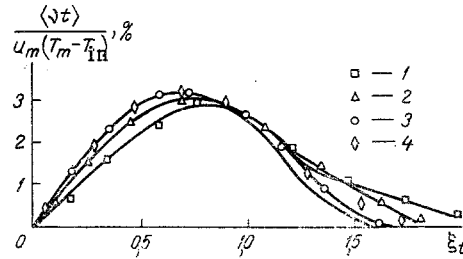


Fig. 2. Transverse heat flux: 1) $x/d = 20$; 2) 40; 3) 60; 4) 100.

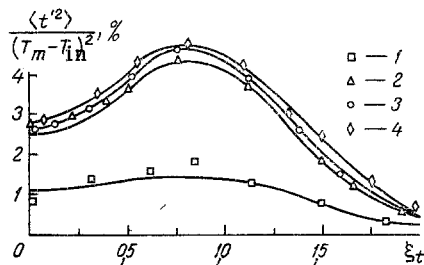


Fig. 3

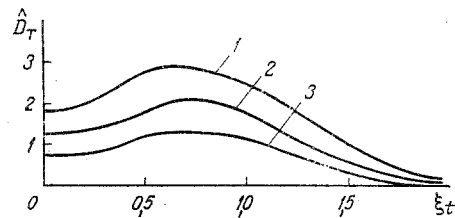


Fig. 4

Fig. 3. Mean square temperature fluctuations: 1) $x/d = 20$; 2) 40; 3) 60; 4) 100.

Fig. 4. Dissipation rate of temperature pulsations: 1) $x/d = 20$; 2) 60; 3) 100.

In solving the problem, numerical modeling is undertaken: the dependence of the numerical results on the model used to describe the jet is investigated, phenomenological constants of the system of equations that are optimal from the viewpoint of agreement with experiment are sought, various difference schemes are considered, allowing, above all, the accuracy and speed of calculation to be increased, and the dependence of the computational results on the choice of initial and boundary conditions is analyzed.

Results of the Calculation

1. Analysis of the results of calculation shows that the model used, in combination with an effective numerical algorithm, allows computational data in good agreement with experiment to be obtained in the range of jet cross section 20-100 diameters. The relative error in determining the maximum values of the functions is 3-10% for the dynamic characteristics, while the mean temperature and its mean square pulsations are determined with an accuracy of 5-10%; the corresponding figures for the thermal characteristics are 5-15% and 5-10%.

2. The optimal values of the phenomenological constants, ensuring the best agreement between calculation and experiment, are

$$\begin{array}{lll}
a_1 = 0,027, & b_1 = 0,025, & c_1 = 0,025, \\
a_2 = -0,13, & b_2 = -2,0, & c_2 = -2,85, \\
a_3 = -5,60, & b_3 = -2,0, & c_3 = -3,80, \\
l_1 = 0,11, & l_2 = -0,333, & l_3 = -4,52, \\
m_1 = 0,115, & m_2 = -2,0, & m_3 = -2,0.
\end{array}$$

3. The time to calculate a single variant is 6-10 min on a BESM-6 computer with grid steps $h_x = h_y = 0.1$.

4. The calculated and experimental values of the mean-temperature defect (Fig. 1) for jet cross sections $\hat{x} = 40-80$ diameters are in agreement within the limits of physical error of the measurements (3-8%). The error increases as the cross section approaches the nozzle. When $\hat{x} = 20$, it is 15%.

5. The calculational and experimental results of the transverse heat flux (Fig. 2) agree within the limits of physical error of the measurements close to the axis, but give a relative error of the order of 50% close to the boundary. When $\xi_t \leq 0.8$, the normalized flux is smaller for smaller cross sections; when $\xi_t \geq 1.0$, the opposite is true.

6. The normalized mean-square temperature pulsations (Fig. 3) agree with experiment within the limits of physical error of the measurements. The maximum value of the normalized pulsations increases with increase in distance from the nozzle. The greatest deviation from experiment is observed at distances $\hat{x} = 20-30$ diameters from the nozzle.

7. The variation in dissipation rate of the temperature pulsations is shown in Fig. 4. The lack of experimental data prevents a comparison.

LITERATURE CITED

1. R. A. Antonia, *Int. J. Heat Mass Transfer*, 28, No. 10, 1805-1812 (1985).
2. B. E. Launder, *Topics in Applied Physics*, Springer, Berlin (1976), pp. 231-287.
3. E. V. Radkevich, in: *Application of Mathematical Methods and Computational Techniques in Solving Economic Problems* [in Russian], Gomel' (1986), p. 255.
4. V. N. Abrashin, V. N. Barykin, and E. V. Radkevich, *Algorithm and Some Results of Calculating Plane Isothermal Gas Jet*. Preprint No. 22 [in Russian], Institute of Mathematics, Academy of Sciences of the Belorussian SSR, Minsk (1986).

INFLUENCE OF THE VELOCITY PROFILE ON THE HEAT TRANSFER OF A CIRCULAR IMPACT JET

A. I. Abrosimov and A. V. Voronkevich

UDC 536.242:532.525.2

The influence of the mean velocity profile in a round submerged jet on the heat transfer with a plane obstacle placed along the normal to the flow is investigated. A criterial relation for the heat transfer in the vicinity of the critical point is obtained.

The interaction of an immersed impact jet with a uniform velocity profile at the nozzle outlet and a low level of initial turbulence ϵ_0 with an obstacle is characterized by maximum effectiveness of heat transfer at a distance of $h = 7-8$ in the vicinity of the critical point of the obstacle [1]. This has been noted in many works. In [2], it was suggested that the presence of a peak of the heat-transfer coefficient in the vicinity of the critical point is a result of the combined influence of increase in intensity of turbulence at the jet axis ϵ_m and decrease in the axial velocity in the transitional section of the jet.

All-Union Scientific-Reserach Institute of Electromechanics, Istra. Translated from *Inzhenerno-Fizicheskii Zhurnal*, Vol. 54, No. 3, pp. 393-398, March, 1988. Original article submitted November 12, 1986.